Robotica: page 1 of 18. © Cambridge University Press 2014
doi:10.1017/S026357471300129X

Development of a two-wheel mobile manipulator: balancing and interaction control

Jae Kook Ahn and Seul Jung*

Intelligent Systems and Emotional Engineering Laboratory, Department of Mechatronics Engineering, Chungnam National University, Dajeon, Korea

(Accepted December 12, 2013)

SUMMARY
This paper focuses on practical application of a mobile manipulator by presenting the development and control of a two-wheel mobile robot with two arms called a balancing service robot (BSR) designated for indoor services. The mobile manipulator requires not only robust balancing position control but also force control to interact with objects. Movements with two wheels are controlled to satisfy stable balancing control for navigation and manipulation with two arms to perform given tasks. The robot is required to deal with external forces to maintain balance. The position-based impedance force control method (the admittance control) is utilized by filtering the force with the impedance function to react to the applied force from the operator. Experimental studies of navigation control under balancing condition and interacting control with a human operator are demonstrated. Experimental results confirm that the robot has smooth reaction against the disturbance induced by the applied external force.

KEYWORDS: Control of robotic systems; Force control; Service robots; Mobile robots; Mechatronic systems.

1. Introduction

The mobile manipulator is a complex system that combines two systems, a mobile robot and manipulators. The mobility is not enough for mobile robots to perform tasks such as handling, manipulating, and assembling, namely, tasks requiring contact with objects beyond surveillance. Adding the manipulability to the mobility increases degrees-of-freedom (DOF) of mobile robots to the maximum of having infinite workspace. Not only navigation but also manipulation is feasible in the framework of mobile manipulators. Although the corresponding dynamics and control of the mobile manipulator become complicated, the feasibility can be maximized in the practical point of view.

Many different types of mobile manipulators have been presented.[1–8] Two arms on Segway form an astronaut robot for a spacecraft,[1] and one arm or a body on two wheels form the mobile inverted pendulum structure.[2,3] Cooperative control of two mobile manipulators has been presented.[9–11] However, mobile manipulators with two arms instead of a single arm are more feasible in the sense of task-oriented environment due to more DOFs to handle objects properly. Controlling mobile manipulators has to deal with coupled movements between mobile robot and arms in which arm movements can be constrained. The mobility of mobile platforms can solve kinematics constraints of the manipulator in their work space by adding another DOF.

Thus, the home service robot should be a form of the mobile manipulator whose structure includes two arms and a mobile base. TWENDY-ONE is built as a typical home service robot that can manipulate objects with two arms in home environment.[12] For sophisticated manipulation tasks, door opening control of a service robot has been presented.[13]

To perform aforementioned tasks in the home environment, the robot is required to have not only position control but also sophisticated force control for successful interaction.[14–16]

* Corresponding author. E-mail: jungs@cnu.ac.kr

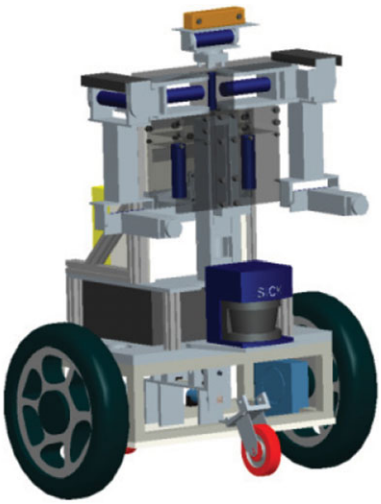

Fig. 1. (Colour online) Schematic design of a balancing service robot.

Two arm coordination control using internal impedance control method has been successfully demonstrated.[17–19]

Constrained interaction between robot and human is addressed for assembly task and contact analysis.[20–23] In other aspect, interaction between human and robot can also be performed without touching each other.[24–26] Stable motion control by using a disturbance observer under external force has been demonstrated.[3] Two mobile manipulators have been developed to dance together and their performances have been demonstrated to confirm force control methods.[27]

Recently, mobile manipulators have been equipped with two wheels for challenging control tasks.[1–3,28–31] A two-wheel limbo robot has been presented for limbo dance based on planning and control to demonstrate robust balancing control.[31]

However, interaction control of two-wheel mobile manipulators with other objects has not been addressed in the literature yet except the authors in ref. [32]. To perform the interaction control for BSR, not only balancing control but also force control is required. Balancing control should be completely accomplished *a priori* before applying force control.

In this paper, a mobile manipulator with the balancing mechanism has been designed and implemented for indoor service applications as an extension of the paper.[32] The robot has several interesting characteristics in the design points of view as shown in Fig. 1. Firstly, the robot has two driving modes: one is the balancing mode that the robot can balance itself with two wheels and another mode is a wheeled drive mobile mode with two wheels and two casters. Secondly, the height of the balancing service robot (BSR) can be adjusted by using a linear motion at the waist. Lastly, the structure of the robot can be separated in two parts, an upper arm body and a lower mobile base. The separable body structure is convenient for a mobile base to perform a cleaning task independently.

In accordance with design characteristics, balancing and interaction control of BSR are empirically conducted to prove the functionality of hardware implementation as well as control algorithms. Experimental studies of a mobile manipulator for balancing control, navigation control, and interaction control are presented and analyzed for feasible applications.

2. Modeling and Control scheme

The kinematics of BSR is analyzed and simulated. Linear controllers are designed for the balancing control performance. Force control for interaction is augmented with position control.

2.1. Modeling of balancing service robot

The BSR shows the combined structure of two systems: a mobile robot system and an inverted pendulum system. Thus, the robot can navigate on the plane like a mobile robot while balancing like an inverted pendulum system. One of advantages of the mobile inverted pendulum structure is the mobility which allows the robot to turn in the narrow space.

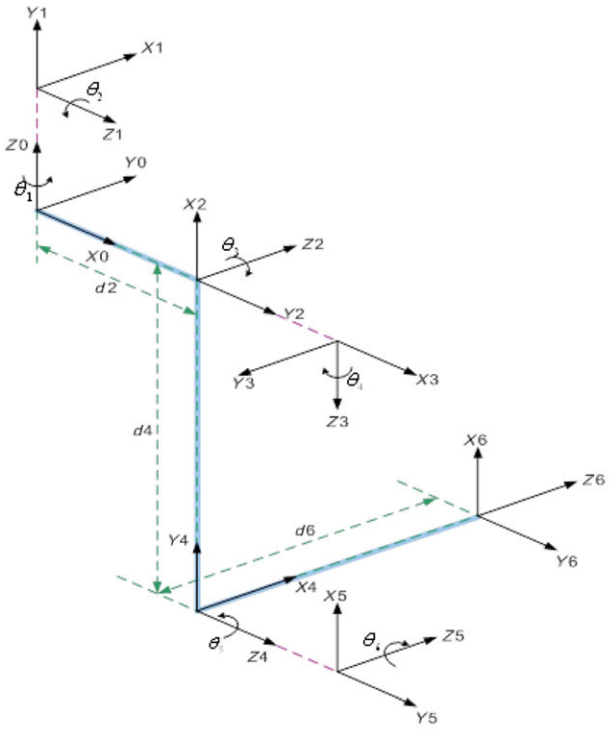

(a) Coordinate based on D-H parameter of one arm

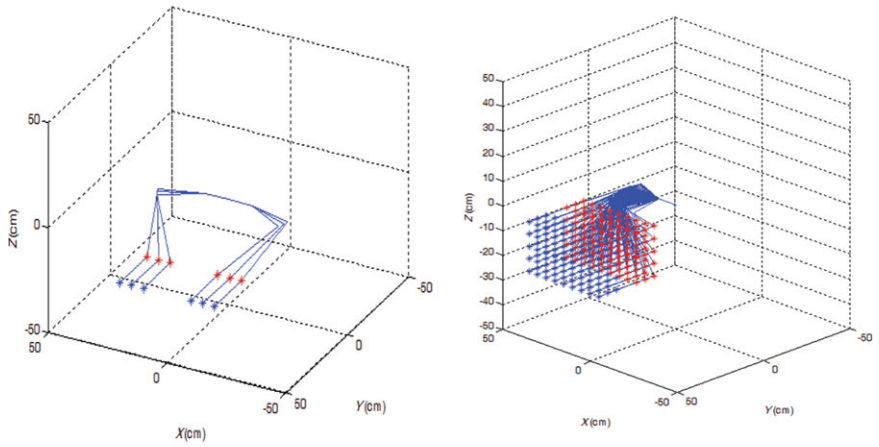

(b) Position by forward and inverse kinematics

Fig. 2. (Colour online) Robot arm Kinematics simulation.

For the robot arm, forward and inverse kinematics equations are derived based on the coordinate shown in Fig. 2 (a).[33] The detailed kinematics equations including D-H parameters are given in ref. [33]. Simulation studies of testing forward and inverse kinematics equation are shown in Fig. 2 (b). Figure 2 shows the solutions of the forward and inverse kinematics together, which matches exactly.

The orientation of the mobile robot can be considered as a rotational matrix.

$$T_{z,\phi} = \begin{bmatrix} \cos\phi & -\sin\phi & 0 & 0 \\ \sin\phi & \cos\phi & 0 & 0 \\ 0 & 0 & 1 & d_z \\ 0 & 0 & 0 & 1 \end{bmatrix} \tag{1}$$

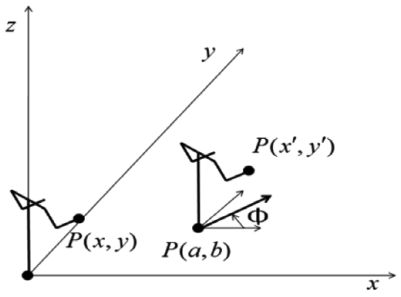

Fig. 3. Coordinates of BSR.

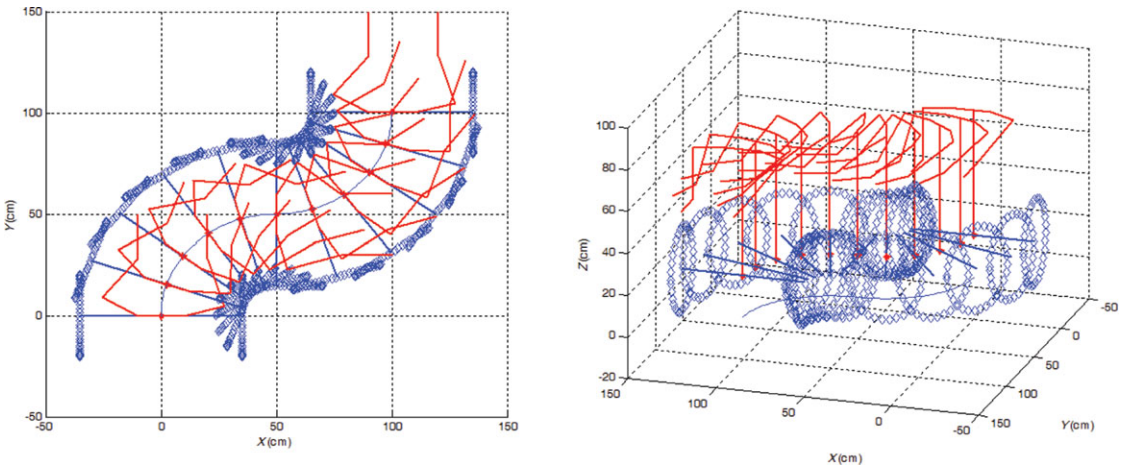

Fig. 4. (Colour online) BSR Kinematics simulation.

where d_z is the distance from the mobile base to the origin of the manipulator and ϕ is the heading angle of the mobile base. Then the matrix in Eq. (1) can be combined with the transformation matrix of the manipulator ${}^0T_6$ found in ref. [33].

From the mobile base to the manipulator, the kinematics can be described as:

$$ {}^BT_6 = T_{z,\phi}\,{}^0T_6 \tag{2}$$

When the robot moves from the Cartesian position $P(x, y)$ to $P(x', y')$ on the plane as described in Fig. 3, the new position can be obtained as:

$$ P(x', y') = P(x + a, y + b) \tag{3}$$

Simulations on kinematics (2) and (3) based on the movements of a mobile manipulator have been carried out and shown in Fig. 4. Figure 4 shows trajectories of a mobile manipulator from (0,0) to (100,100) based on the kinematics. Simulation results confirm the kinematics of Eqs. (2) and (3).

For the balancing control, the robot in Fig. 1 can be simply modeled as a mobile inverted pendulum structure as shown in Fig. 5. The goal of BSR is to regulate the balancing angle, θ, the heading angle, ϕ, and the position, p by two wheel velocities $\dot{\theta}_R, \dot{\theta}_L$, induced from torque inputs, τ_R, τ_L, respectively.

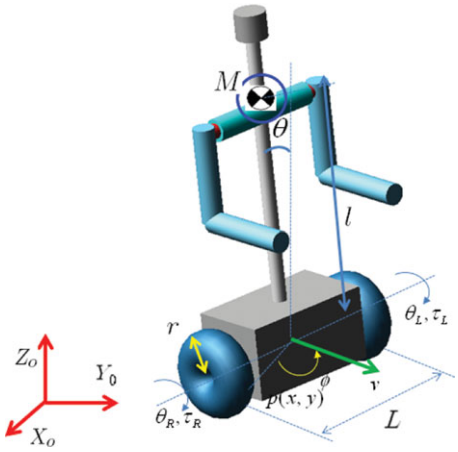

Fig. 5. (Colour online) Modeling of balancing service robot.

The motion kinematics equation of the mobile base can be represented between joint velocities $\dot{\theta}_R, \dot{\theta}_L$ and the Cartesian velocities $\dot{x}, \dot{y}, \dot{\phi}$ under the assumption that the center of gravity is located on the wheel axis.[2,35]

$$\begin{bmatrix} \dot{x} \\ \dot{y} \\ \dot{\phi} \end{bmatrix} = \begin{bmatrix} \frac{r}{2}\cos\phi & \frac{r}{2}\cos\phi \\ \frac{r}{2}\sin\phi & \frac{r}{2}\sin\phi \\ \frac{r}{L} & -\frac{r}{L} \end{bmatrix} \begin{bmatrix} \dot{\theta}_R \\ \dot{\theta}_L \end{bmatrix} \tag{4}$$

where r is the radius of the wheel and L is the distance between two wheels.

Differing wheel velocities can generate movements of the robot on the plane. Thus, a torque input to each wheel can ultimately control the Cartesian motion of the robot. This is known as a kinematics-based control scheme. Since movements of two arms have influences on the balancing mechanism of the robot, balancing control must be robust enough. Balancing control of two-wheel mobile robots has been demonstrated.[29,30]

2.2. Balancing and navigation control

For the successful position control of BSR, three control variables such as a balancing angle, an orientation angle and a position should be considered simultaneously for navigation control performance. A PD control method is used for the balancing angle control while PID controllers are used for the orientation angle control as well as the position control.[29,30,32] The reason of using PD control instead of PID for the balancing angle is to reject the effect of accumulated errors by integration due to the balancing angle error without knowing the center of gravity of the system.[34,35]

The torque of the right wheel τ_R and the torque of the left wheel τ_L are described as a sum of each controller output such as the balancing angle controller output u_θ, the heading angle controller output u_ϕ, and the position controller output u_p.

$$\begin{aligned} \tau_R &= u_\theta + u_p + u_\phi \\ \tau_L &= u_\theta + u_p - u_\phi \end{aligned}. \tag{5}$$

Each variable is controlled by linear controllers as below.

$$\begin{aligned} u_\theta &= K_{p\theta}(\theta_d - \theta) + K_{d\theta}(\dot{\theta}_d - \dot{\theta}) \\ u_p &= K_{pp}(p_d - p) + K_{ip}\int (p_d - p)\mathrm{d}t + K_{dp}(v_d - v), \\ u_\phi &= K_{p\phi}(\phi_d - \phi) + K_{i\phi}\int (\phi_d - \phi)\mathrm{d}t + K_{d\phi}(\omega_d - \omega), \end{aligned} \tag{6}$$

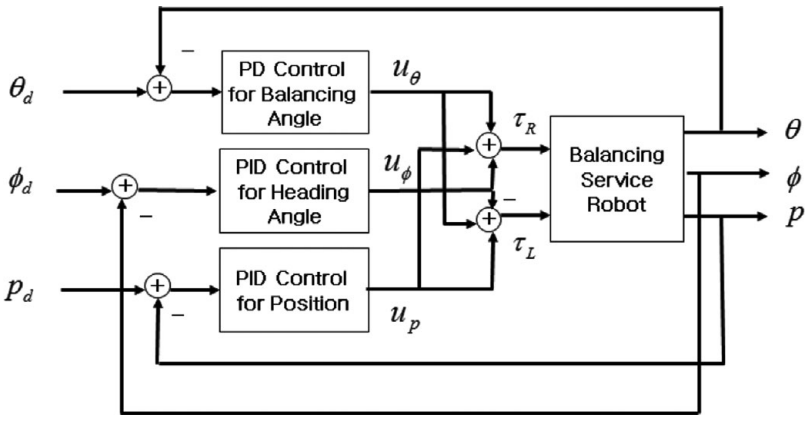

Fig. 6. Position control of balancing service robot.

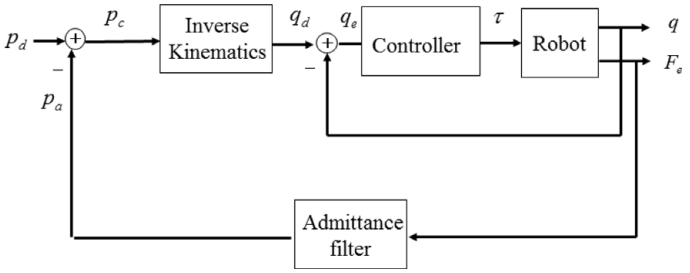

Fig. 7. Force control structure.

where $K_{d\theta}$, $K_{p\theta}$ are the controller gains for the balancing angle, K_{pp}, K_{dp}, K_{ip} are the controller gain for the position, and $K_{p\phi}$, $K_{i\phi}$, $K_{d\phi}$ are the controller gains for the heading angle.

The control block diagram for the mobile base is shown in Fig. 6.

2.3. Interaction force control

Robot arms are designed to perform manipulation tasks. Each arm has 6 DOF. The left arm has a force sensor attached to the end effector to have the interaction capability. Interaction between BSR and an operator can be accomplished by the force control which has been known as a sophisticated algorithm. Applied force can be regulated by indirect filtering of an impedance force control method, which is known as one of major force control algorithms.

Different from the torque-based impedance control,[14–18] the external force induced by an operator is filtered through the admittance function and compared with the desired Cartesian trajectory to generate the positional error. Then the positional error becomes the modified Cartesian trajectory to be converted to the desired joint position through inverse kinematics for the robot to follow. This is known as the position-based impedance control (the admittance control).

In the framework of the position-based impedance control, dual control loops are used as shown in Fig. 7. The inner position loop is controlled for the joint position control by PID controllers and the outer loop is used for force control. The external force plays a role of modifying the desired trajectory for the robot to react through the impedance relationship.[34]

The commanded force, F_e by the operator passes through the admittance filter and converted into the position adjustment vector, P_a.

$$F_e = M\ddot{P}_a + B\dot{P}_a + KP_a, \tag{7}$$

where $M, B, K \in R^{n\times n}$ are impedance parameter matrices of mass, damping, and stiffness, respectively. The Cartesian position reference, P_r is modified to P_c in terms of P_a. The adjustment position, P_a can be obtained from the admittance filter.

Fig. 8. (Colour online) Real balancing service robot.

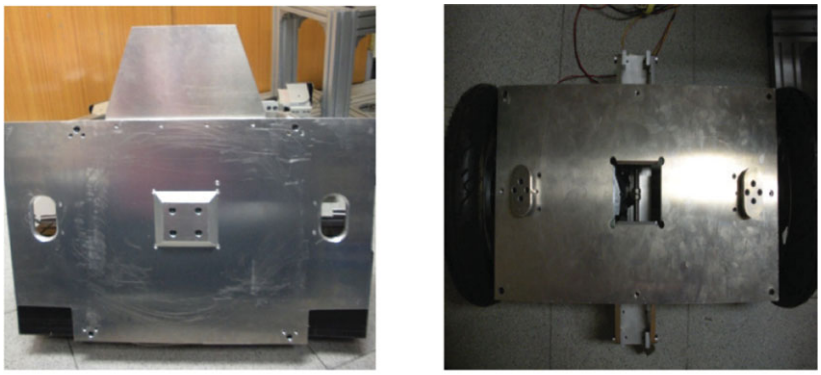

(a) Bottom of Upper body (b) Top of lower wheels

Fig. 9. (Colour online) Separable structure.

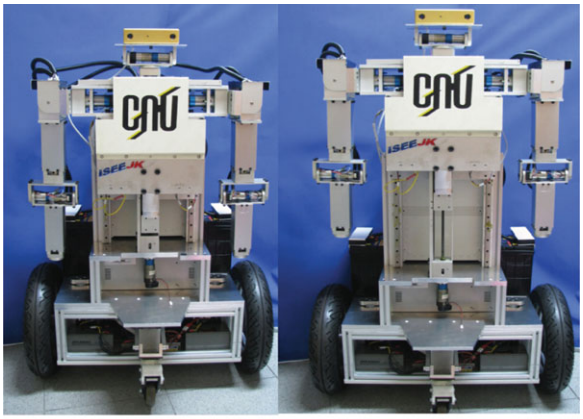

(a) Normal (b) Stretched

Fig. 10. (Colour online) Height controllable waist structure.

For simplicity, the *i*th directional force, f_{ei} induced by the operator can be transformed as:

$$p_{ai}(s) = \frac{1}{m_i s^2 + b_i s + k_i} f_{ei}(s), \tag{8}$$

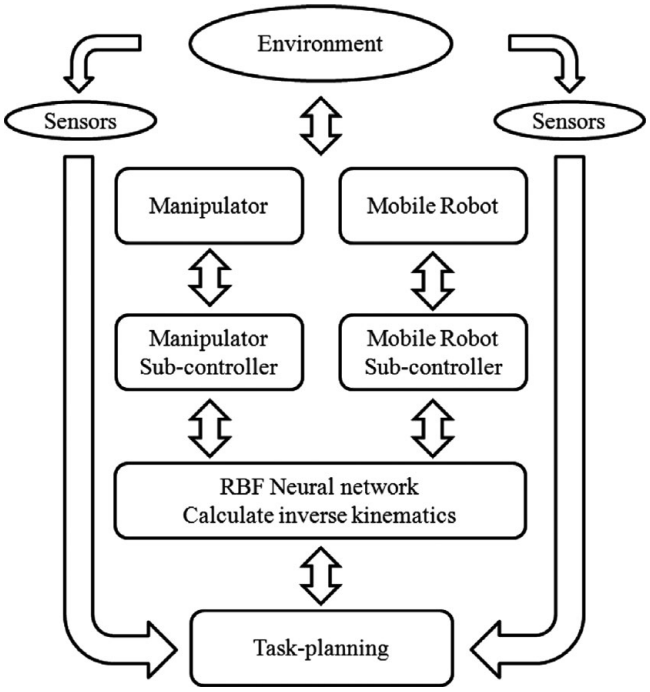

Fig. 11. Overall system structure.

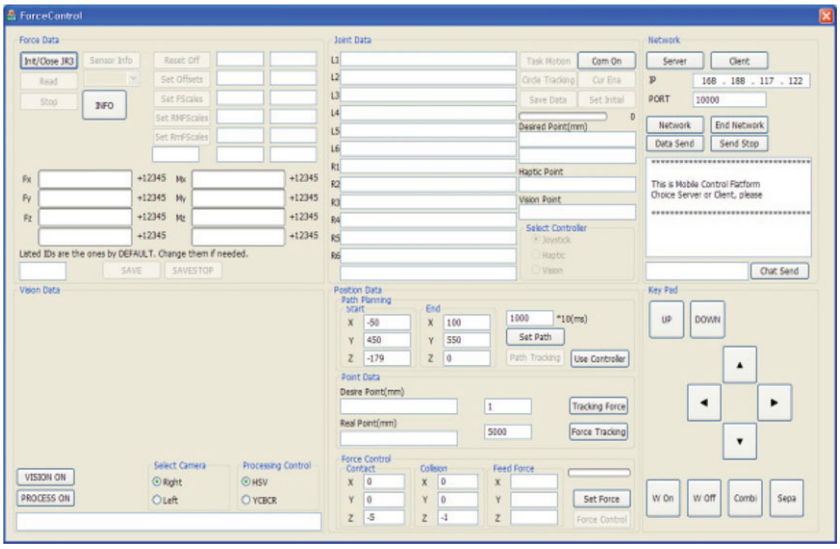

Fig. 12. (Colour online) GUI Panel.

where s is the Laplace operator and m_i, b_i, k_i are impedance parameters. The force contribution is transformed into the trajectory so that the reference trajectory is modified as:

$$p_{ci} = p_{ri} - p_{ai}, \tag{9}$$

where p_{ci} is the modified Cartesian trajectory due to the interaction force, f_{ei}. The modified Cartesian trajectory, p_{ci} is transformed to the desired joint value, q_{di} through the inverse kinematics. Then the inner loop controls the joint trajectory, q_i to track the desired joint trajectory, q_{di}. This forms the position-based impedance control scheme. This same idea can be extended to multiple input forces to multiple joints.

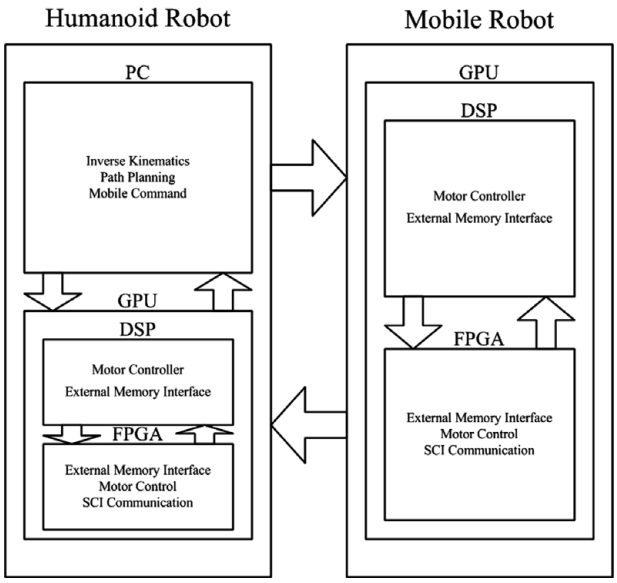

Fig. 13. Control hardware structure.

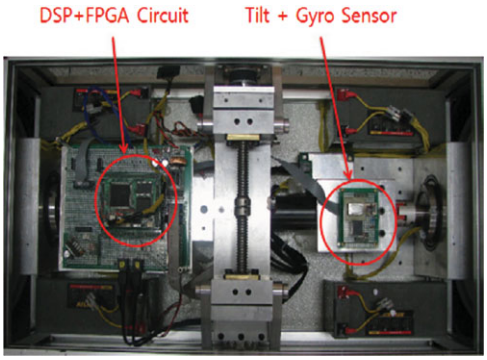

Fig. 14. (Colour online) Base wheel control hardware.

3. Balancing Service Robot

3.1. Real balancing service robot

The real BSR is designed and implemented as shown in Fig. 8. BSR consists of a base with two wheels, an upper body with two arms, a stretchable waist, a head with camera, and a computer. A force sensor is mounted at the end of the left arm. The laser sensor is located at the front to detect obstacles. A stereo camera is located on the head.

The base wheels have two casters to maintain stable contact on the ground at the beginning. The caster lifting mechanism enables casters to be lifted up so that the robot becomes the balancing mode with stability.

3.2. Design characteristics

The BSR has three notable characteristics in the mechanical design points of view. The robot has the separable body structure such that upper body arms and lower base wheels can be separated in two parts. This structure allows the base wheels to navigate itself alone for the cleaning purpose.

Figure 9 shows the connecting part of two separable bodies: (a) bottom of upper body arms and (b) top of lower base wheels. Connecting parts are passively separated at this moment, but they will be automatically separated in the future after redesigning the system.

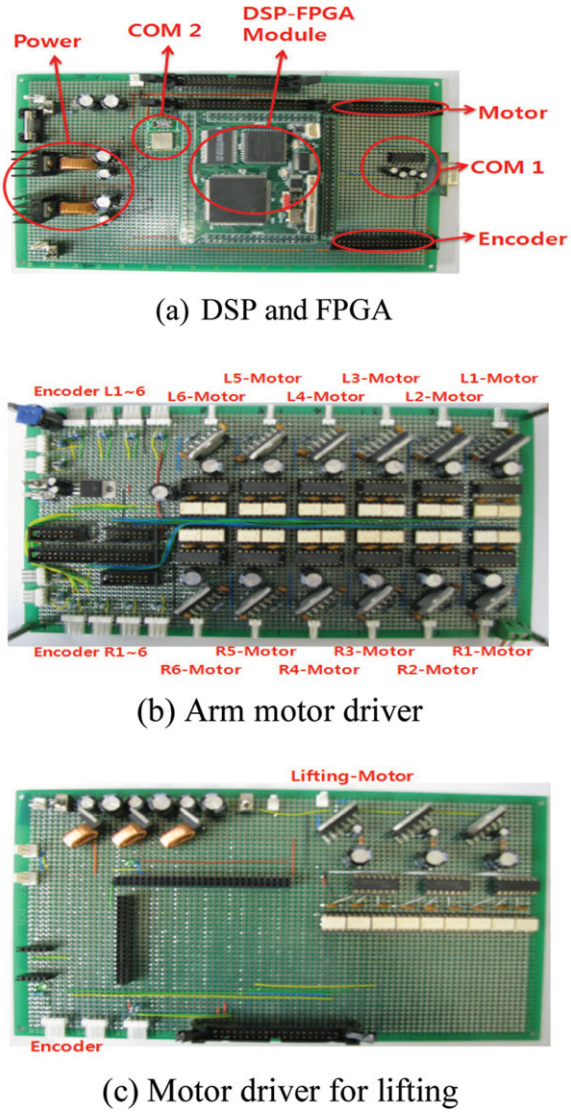

Fig. 15. (Colour online) Upper arm control hardware.

Another interesting characteristic of the BSR is the stretchable waist. The waist has the lifting mechanism that can lift up the upper body as shown in Fig. 10. A dc motor controls the movements of the guide to lift the upper body arms. After being stretched to the end, the height of the robot gains about 20 cm so that the overall height of the robot becomes 1.3 m from 1.1 m.

The last one is balancing mechanism that allows two driving modes: a balancing mode with two wheels and a mobile robot mode with two wheels and two casters.

3.3. Control environment

Figure 11 shows the overall control environment of the BSR system. Sensors detect information of the robot and measure force from the environment. A computer is the main controller to handle vision processing, sensor fusion, control algorithms, communication with outer devices, and actuations.

Neural network control algorithm of using Radial basis function network is also embedded in the computer to compensate for position errors due to uncertainties along with linear controllers.[36] External force data from the force sensor are used in the computer to command the position of the robot.

Table I. Controller gains.

	Balancing angle, θ	Yaw angle, ϕ	Position, p
k_p	58	50	45
k_i	0	0.5	0.1
k_d	19	3	9

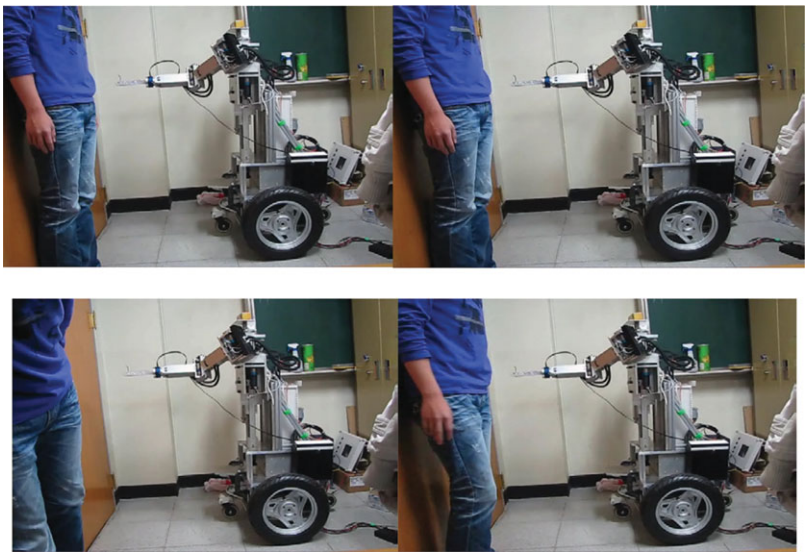

Fig. 16.(Colour online) Balancing control demonstration.

In order for the convenient interface with BSR, GUI is designed to communicate with BSR as shown in Fig. 12. Position and force data are collected and camera image can be displayed in the GUI. Movements of BSR can be controlled by icons in GUI as well.

3.4. Control hardware

3.4.1. Overall structure. The high level control is performed by a PC and low level control is done by DSP and FPGA chips. The upper arms and the lower wheels have independent hardware structures so that they can be separately controlled. A PC as a supervisory controller on the upper arms communicates with DSPs and FPGAs for controlling arms as well as wheels.

The overall control structure is shown in Fig. 13. Each part has a pair of a DSP and an FPGA chip as a local controller. DSP calculates PID control algorithms and FPGA takes care of encoder sensor data and generates PWM control for motors. Efficiency of using FPGA for fan-outs has been addressed in the paper.[36]

3.4.2. Mobile robot control hardware. Figure 14 shows the inside of the base of the wheeled mobile robot. Two dc motors are directly connected to the wheels. DSP and FPGA are located at the left side and sensors to detect a balancing angle are located on the wheel axis for more accurate sensing. Encoders attached to wheels count rotation of wheels to calculate position and orientation through dead-reckoning. Gyro and tilt sensors are used to detect the balancing angle by fusing two sensors through the complimentary filter since cost effective sensors are used instead of expensive ones.[35]

3.4.3. Manipulator control hardware. Figure 15 shows the control hardware for the upper arms. Since each arm has 6 DOF, 12 motor drivers are used to actuate dc motors and regulated by a DSP and an FPGA chip.[36] Encoder data are collected by the FPGA and counted. Then DSP and FPGA share data on external memory through communication.

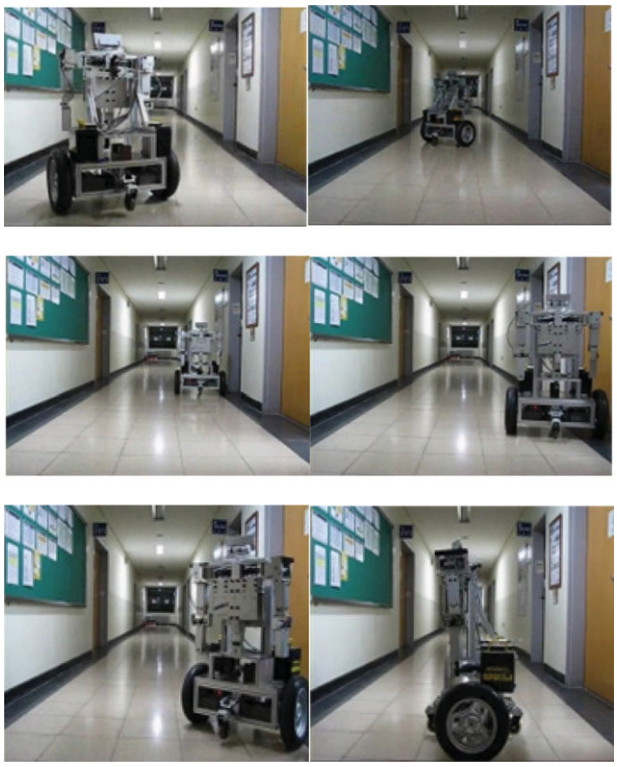

Fig. 17. (Colour online) Balancing control demonstration.

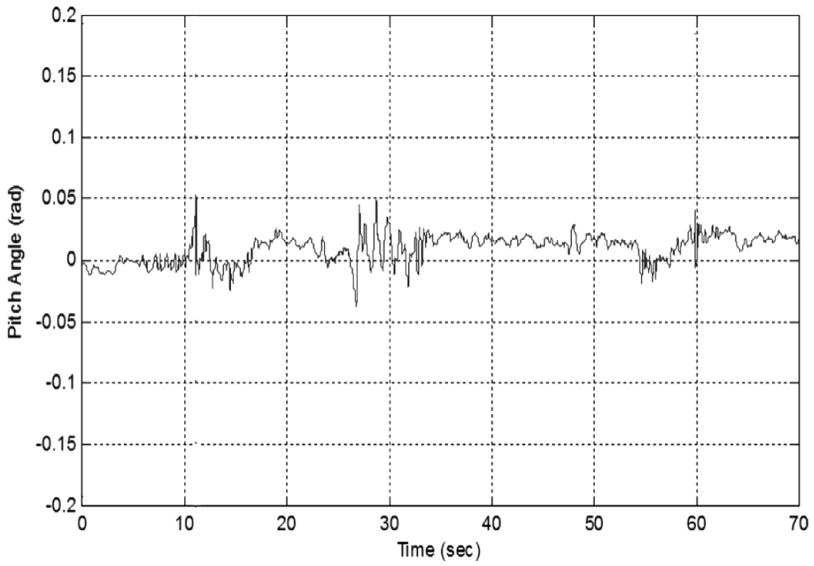

Fig. 18. Balancing angle of Fig. 17.

4. Experimental Studies

BSR is tested and evaluated empirically for the performances of a balancing task, navigation control while balancing, a door opening task, and interaction control with a human operator.

4.1. Balancing control

The robot has two driving modes, a mobile robot mode and a balancing mode. The mobile robot mode uses casters to make contact with the ground for stable driving. The balancing mode does not

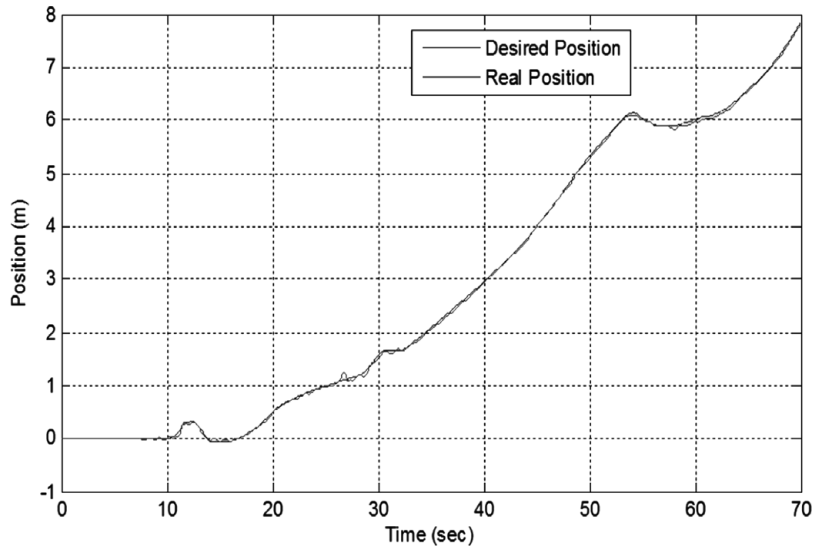

Fig. 19. Position of Fig. 17.

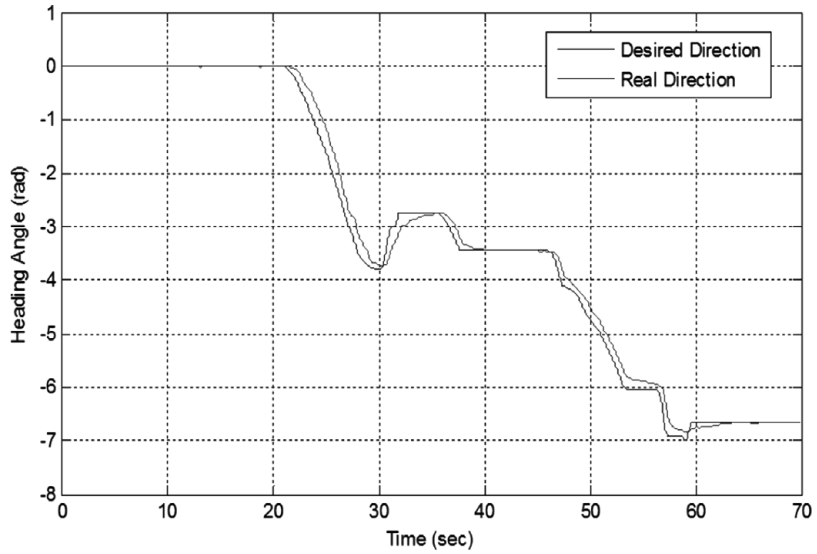

Fig. 20. Heading angle of Fig. 17.

use casters so that the robot has to balance with two wheels. Transition from the mobile robot mode to the balancing mode or vice versa can be achieved by controlling up and down movements of casters.

Firstly, the robot is tested for balancing angle control without moving. The robot has to maintain balancing by itself after casters are lifted up. Figure 16 demonstrates that the robot is maintaining balance well. Without touching the robot, the robot successfully maintains balance.

4.2. Navigation control while balancing

Secondly, the robot is required to navigate indoor environment through wireless communication control. The robot is commanded to follow the desired trajectory given by a remote controller. Initially, the robot is in the mobile mode that maintains stable contact with the ground. Then the robot becomes the balancing mode that balances with two wheels.

Control sampling time is 100 Hz and controller gains are listed in Table I.

The robot is required to follow the commanded trajectories, go straight, make turn, and come back. Figure 17 shows the actual movement on the floor. The total traveling time is 70 s. The robot successfully maintains balance within the error of 0.05 radian (2.87°) while traveling around as shown

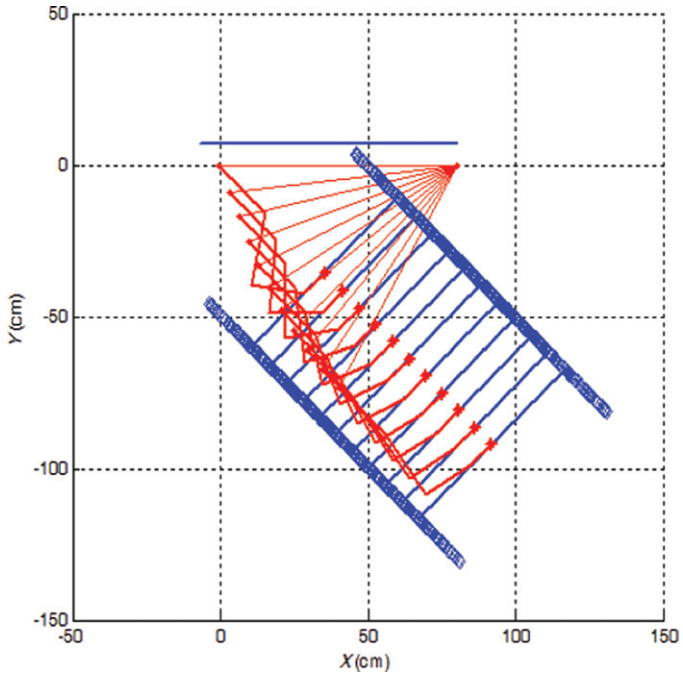

Fig. 21. (Colour online) Trajectory for door opening task.

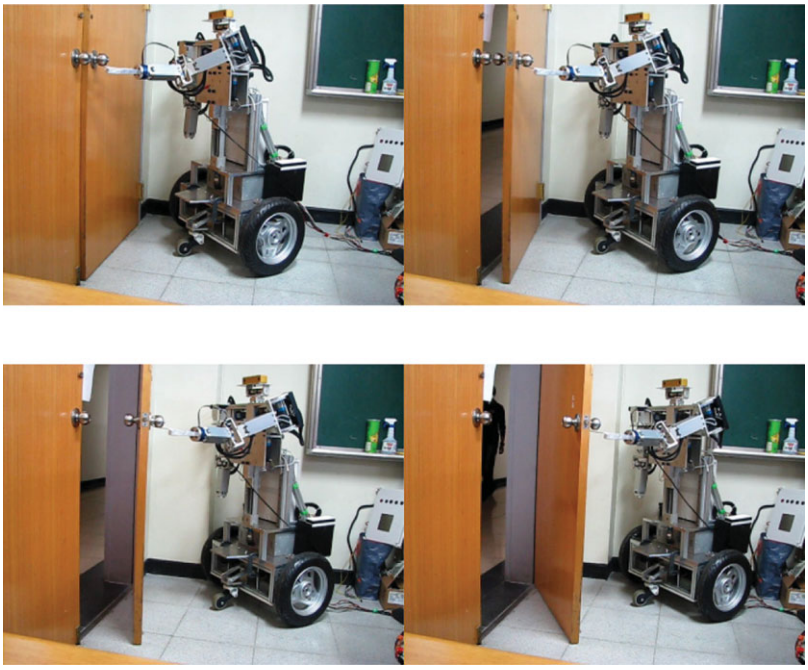

Fig. 22. (Colour online) Door opening task.

in Fig. 18. The traveling distance and the heading angle are shown in Figs. 19 and 20 in the local coordinates, respectively.

4.3. Door opening task

The next experiment is the door opening control task by the mobile manipulator. The purpose of this task is to see the advantage of the mobile manipulator that cooperates between robot arms and the mobile base. When the robot opens the door, robot arms have limitation due to length and workspace. The mobile base should help to move back for the manipulator to open the door.

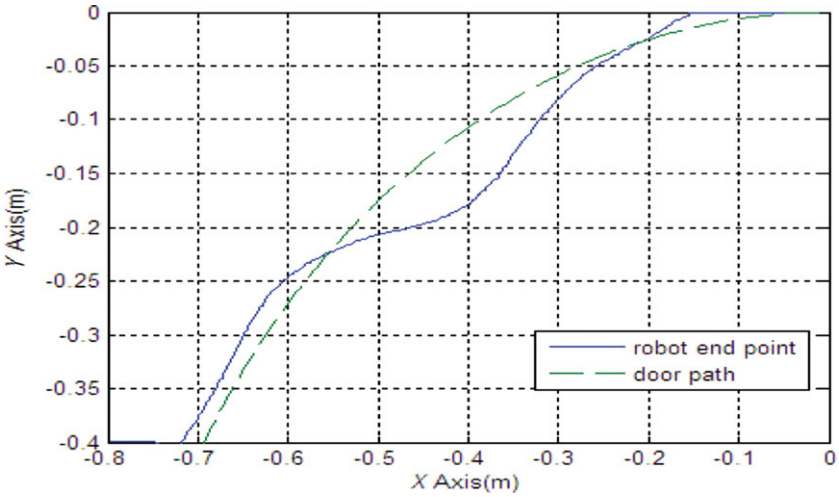

Fig. 23. (Colour online) Trajectory of robot movement for a door opening task.

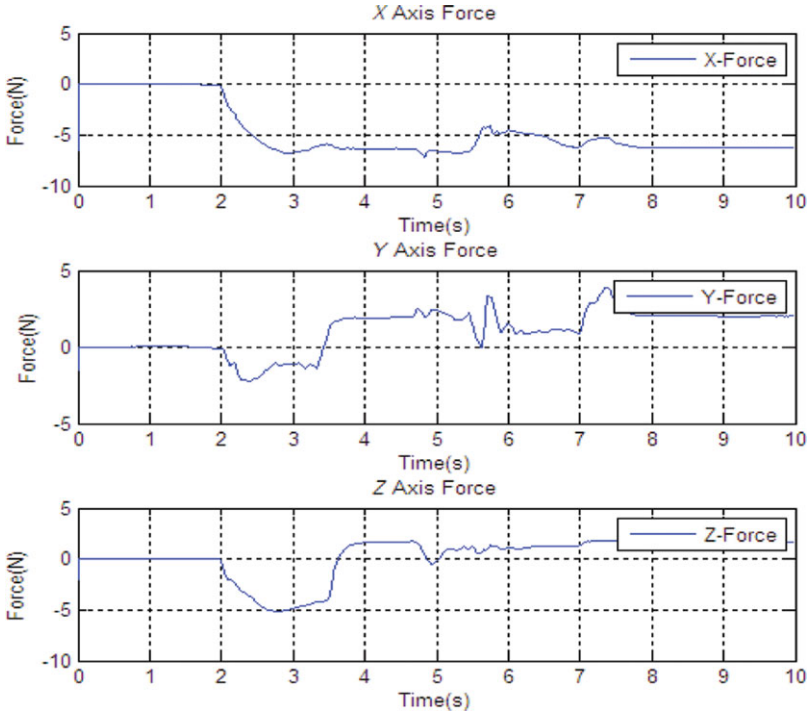

Fig. 24. (Colour online) Forces for door opening task.

First, the trajectory for the robot is generated in off-line fashion as shown in Fig. 21. Then an actual door opening task is conducted. Figure 22 demonstrates that the manipulator opens the door while the mobile base moves back. The corresponding movement and forces for each axis are plotted in Figs. 23 and 24, respectively.

4.4. Interaction control

The final experiment is the interaction control between a human operator and the robot while the robot maintains balancing. The human operator holds the robot arm and pushes and pulls back and forth in one direction. Then BSR reacts to move back and forth according to the commanded force induced by the human operator. Figure 25 demonstrates the actual interaction control task between the robot and the operator. The operator holds and pulls the manipulator. Then he pushes it and let it balance. And he pulls the manipulator again.

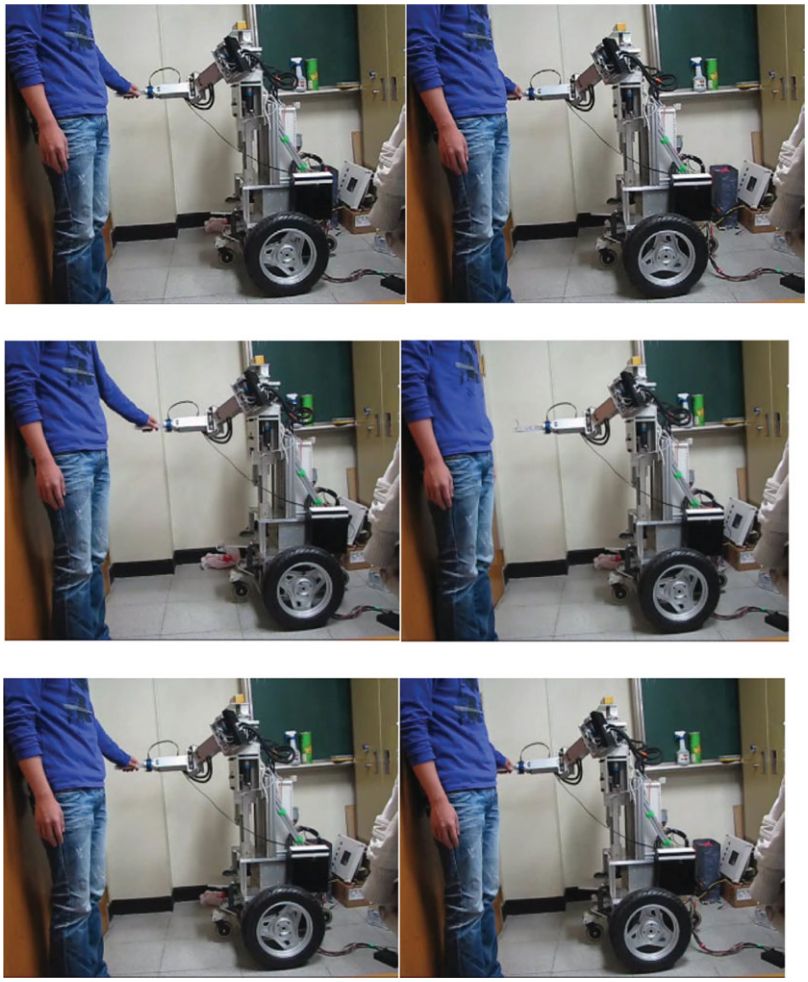

Fig. 25. (Colour online) Interaction force control demonstration.

Figure 26 shows the corresponding plots of Fig. 25. Figure 26(a) shows the balancing angle plot. When the operator pushes and pulls the robot arm, the balancing angle changes with respect to the applied force, but it comes back to zero when it is released. Figure 26(b) shows the applied force to the robot, which is converted to the desired command for the robot to follow. The sign of the external force indicates the push or pull operation. Figure 26(c) shows the corresponding moving distance. The position plot clearly shows the operation. Initially, the operator pushes the robot until 3 s, then holds it for about 2 s, and finally pulls the robot arm at around 5 s.

5. Conclusion

In this paper, a BSR is designed, implemented, and controlled. The robot with several design characteristics has to deal with external forces to maintain balancing. In addition to position control, the robot also has the force control capability to react the external force applied by a human operator. The regulation of the interaction force between the robot and the operator has been confirmed by experimental studies. Interaction force is eventually regulated by the modification of the desired trajectory through filtering of the induced force by a human operator so that the robot can maintain balancing.

Since the bandwidth of the robot for force application is small; however, there is a limitation to the fast movement such that stable reaction to fast external forces sometimes fails. To remedy the failure of balancing mechanism by external forces is one of future research topics. In addition, the

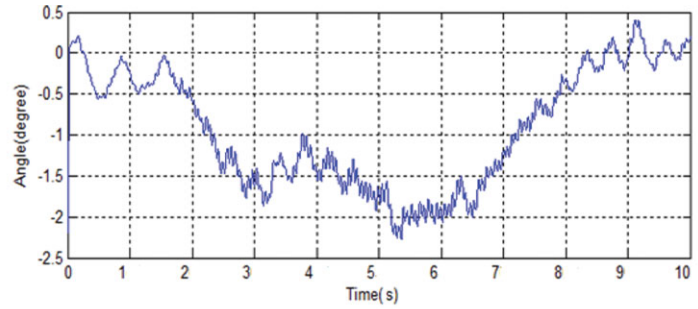

(a) Angle of the balancing robot

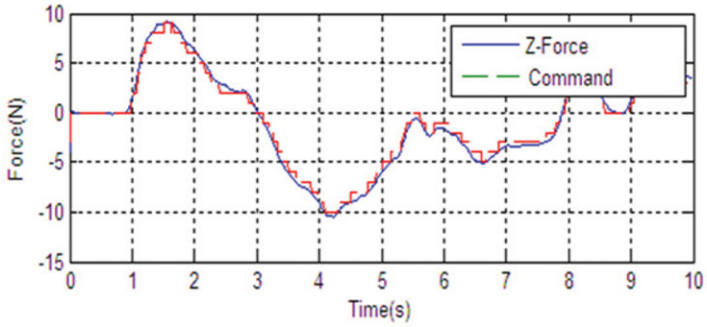

(b) Force of balancing robot

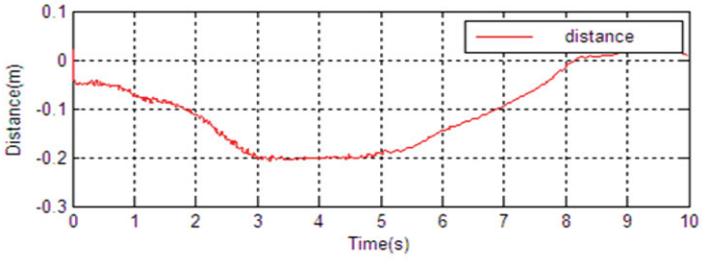

(c) Position of the balancing robot

Fig. 26. (Colour online) Plots of interaction with the Balancing robot in Fig. 25.

robot has to be modified to have automatic separable structure instead of the passive structure. And coordinated manipulation control by two arms while in balancing motion will be investigated.

References

1. R. O. Ambrose, R. T. Savely, S. M Goza, P. Strawser, M. A. Diftler, I. Spain and N. Radford, "Mobile Manipulation Using NASA's Robonaut," *IEEE ICRA*, New Orleans, USA (2004) pp. 2104–2109.
2. S. H. Jeong and T. Takayuki "Wheeled Inverted Pendulum Type Assistant Robot: Design Concept and Mobile Control," *IEEE IROS*, San Diego, USA (2007) pp. 1932–1937.
3. P. K. Abeygunawardhana and T. Murakami, "Environmental Interaction of Two Wheeled Mobile Manipulator by Using Reaction Torque Observer," *IEEE Workshop on Advanced Motion Control*, Trento, Italy (2008) pp. 348–353.
4. C. Ding, P. Duan, M. Zhang and H. Liu, "The Kinematics Analysis of a Redundant Mobile Manipulator," *IEEE Conference on Automations and Logistics*, Qingdao, China (2008) pp. 2352–2357.
5. Y. Wu and Y. Hu, "Output Tracking Control of Mobile Manipulator Via Dynamical Sliding Mode Control," *IEEE Conference on Mechatronics and Automation*, Niagara Falls, Canada (2005) pp. 2160–2164.
6. G. D. White, R. M. Bhatt, C. P. Tang and V. N. Krovi, "Experimental evaluation of dynamic redundancy resolution in a non-holonomic wheeled mobile manipulator," *IEEE/ASME Trans. Mechatronics* **14**(3), 349–357 (2009).
7. D. Xu, D. Zhao, J. Yi and X. Tan, "Trajectory tracking control of omni-directional wheeled mobile manipulators: robust neural network-based sliding mode approach," *IEEE Trans. Syst. Man Cybern.* **39**(3), 788–799 (2009).

8. X. Tan, D. Zhao, J. Yi, Z. G. Hou and D. Xu, "Unified Model and Robust Neural Network Control of Omni-Directional Mobile Manipulators," *IEEE Conference on Cognitive Informatics*, Lake Tahoe, USA (2007) pp. 411–418.
9. K. Sasaki and T. Murakami, "Pushing Operation by Two-Wheel Inverted Mobile Manipulator," *IEEE Workshop on Advanced Motion Control*, Trento, Italy (2008) pp. 33–37.
10. Y. Chen, L. Liu, M. Zhang and H. Rong, "Study on Coordinated Control and Hardware System of a Mobile Manipulator," *World Congress on Intelligent Control and Automation*, Dalian, China (2006) pp. 9037–9041.
11. Z. Li, S. S. Ge and Z. Wang, "Robust adaptive control of coordinated multiple mobile manipulators," *IEEE Conference on Control Applications*, Singapore (2007) pp.71–76.
12. H. Iwata and S. Sugano, "Design of Human Symbiotic Robot TWENDY-ONE," *IEEE International Conference on Robotics and Automation*, Kobe, Japan (2009) pp. 580–586.
13. W. Chung, C. Rhee, Y. Shim, H. Lee and S. Park, "Door opening control of a service robot using a multi fingered robot hand," *IEEE Trans. Ind. Electron.* **56**(10), 3975–3984 (2009).
14. P. W. Jeon, S. Jung and T. C. Hsia, "Contour tracking of an unknown planar object by regulating force for mobile robot navigation " *Robotica* **25**(3), 297–305 (2008).
15. J. Park, D. Hyun, W. H. Cho, T. H. Kim and H. S. Yang, "Normal force control for an in-pipe robot according to the inclination of the pipelines," *IEEE Trans. Ind. Electron.* **58**(12), 5304–5310 (2011).
16. K. Kiguchi and T. Fukuda, "Position/force control of robot manipulators for geometrically unknown objects using fuzzy neural networks," *IEEE Trans. Ind. Electron.* **47**(3), 641–649 (2000).
17. R. Bonitz and T. Hsia, "Robust internal force-based impedance control for coordinating manipulators - theory and experiments," *Int. J. Intell. Mechatronics* **4**(1), 35–67 (Jan. 1999).
18. R. Bonitz and T. Hsia, "Internal force-based impedance control for cooperating manipulators," *IEEE Trans. Robot. Autom.* **12**(1), 78–89 (Feb. 1996).
19. Z. D. Wang, Y. Hirata and K. Kosuge, "Impedance-based Motion Control of Passive-type Robot Porter for Handling an Object," *Proceedings of the 2006 IEEE International Conference on Robotics and Biomimetics*, Kunming, China (2006) pp.709–714.
20. J. Zhang and A. Knoll, "A two-arm situated artificial communicator for human-robot cooperative assembly," *IEEE Trans. Ind. Electron.* **50**(4), 651–658 (2003).
21. G. Grunwald, G. Schreiber, A. Albu-Schaffer and G. Hirzinger, "Programming by touch: The different way of human-robot interaction," *IEEE Trans. Ind. Electron.* **50**(4), 659–666 (2003).
22. H. Iwata and S. Sugano, "Human-robot contact state identification based on tactile recognition ", *IEEE Trans. Ind. Electron.* **52**(6), 1468–1477 (2005).
23. C. Mitsantisuk, S. Katsura and K. Ohishi, "Force control of human-robot interaction using twin direct-drive motor system based on modal space design," *IEEE Trans. Ind. Electron.* **57**(4), 1383–1392 (2010).
24. A. Green and K. S. Eklundh, "Designing for learnability in human-robot communication," *IEEE Trans. Ind. Electron.* **50**(4), 644–650 (2003).
25. K. Morioka, J. H. Lee and H. Hashimoto, "Human-follow mobile robot in a distributed intelligent sensor network," *IEEE Trans. Ind. Electron.* **51**(1), 229–237 (2004)
26. B. Jensen, N. Tomatis, L. Mayor, A. Drygajlo and R. Siegwart, "Robots meet humans-interaction in public space," *IEEE Trans. Ind. Electron.* **52**(6), 1530–1546 (2005).
27. H. Wang and K. Kosuge, "Towards an Understanding of Dancers' Coupled Body Dynamics for Waltz," *IEEE/RSJ International Conference on Intelligent Robots and Systems*, San Francisco, USA (2011) pp. 2008–2013.
28. P. K. Abeygunawardhana and T. Murakami, "Vibration suppression control of two-wheel mobile manipulator using resonance-ratio-control-based null-space control," *IEEE Trans. Ind. Electron.* **57**(12), 4137–4146 (2010).
29. J. S. Noh, G. H. Lee and S. Jung, "Position control of a mobile inverted pendulum system using radial basis function network," *Int. J. Control Autom. Syst.* **8**(1), 157–161 (2010).
30. S. S. Kim and S. Jung, "Control experiment of a wheel-driven mobile inverted pendulum using neural network," *IEEE Trans. Control Syst. Technol.* **16**(2), 297–303 (2008).
31. K. Teeyapan, J. Wang, T. Kunz and M. Stilman, "Robot Limbo: Optimized planning and control for dynamically stable robots under vertical obstacles," *IEEE Conference on Robotics and Automations*, Anchorage, USA (2010) pp. 4519–4524.
32. J. K. Ahn, S. J. Lee and S. Jung, "Force Control Application to a Mobile Manipulator with Balancing Mechanism," *IECON*, Glendale, USA (2010) pp. 1522–1527.
33. D. H. Song, W. K. Lee and S. Jung, "Kinematic analysis and implementation of a motion-following task for a humanoid slave robot controlled by an exoskeleton master robot," *Int. J. Control Autom. Syst.* **5**(6), 681–690 (2007).
34. H. J. Lee and S. Jung, "Guidance control of a wheeled mobile robot with human interaction based on force control," *Int. J. Control Autom. Syst*. **8**(2), 361–368 (2010).
35. H. J. Lee and S. Jung, "Control of a Mobile Inverted Pendulum Robot System," *ICCAS*, Seoul, Korea (2008) pp. 217–222.
36. S. Jung and S. S. Kim, "Hardware implementation of a real-time neural network controller with a DSP and an FPGA for nonlinear systems," *IEEE Trans. Ind. Electron.* **54**(1), 265–271 (2007).